IBM Research Report

Optimized Waveform Relaxation Methods for RC Type Circuits

Martin J. Gander

Dept. of Mathematics and Statistics

McGill University

Montreal, QC, H3A 2K6

Canada

Albert Ruehli

IBM Research Division

Thomas J. Watson Research Center

P. O. Box 218

Yorktown Heights, NY 10598

Research Division
Almaden - Austin - Beijing - Haifa - India - T. J. Watson - Tokyo - Zurich

Optimized Waveform Relaxation Methods for RC Type Circuits

Martin J. Gander
Dept. of Mathematics and Statistics
McGill University
Montreal, QC, H3A 2K6
Canada

Albert Ruehli
IBM Research Division
P.O. Box 218
Yorktown Heights, NY 10598
USA

February 3, 2002

Abstract

Waveform Relaxation has been widely used in circuit theory, for the solution of large systems of ordinary differential equations and the solution of partial differential equations. In the past, clever partitioning schemes have been used for circuit theory applications to enhance convergence. However, a drawback of the classical waveform relaxation algorithm is the non-uniform convergence over the window in time for which the equations are integrated. We propose a new optimized waveform relaxation algorithm which greatly accelerates the convergence by introducing new transmission conditions. These conditions are responsible for the exchange of information between the subcircuits. We use two RC circuit examples to illustrate the theory, as well as the improved convergence behavior.

1 Introduction

The Waveform Relaxation (WR) algorithm was conceived originally [1] to speed up the solution of large circuits as compared to conventional circuit solver methods [2, 3, 4]. After this quite a few circuit solvers and experimental solvers where built based on the WR technique e.g. [5, 6, 7]. One of the most challenging problems in the implementation of the WR algorithm has been the partitioning of the circuits into sub-circuits or subsystems such that the efficiency of the algorithm is maximized e.g. [8, 9, 10, 11]. In this paper we introduce a class of methods which improve the performance over the *classical* WR algorithm with little computational overhead. We call these methods the *optimized* WR algorithms since they involve an optimization process. The optimization concerns what we call the transmission conditions. The function of the tramsmission conditions is to transport information from each subsystem to its connected neighbor subsystems. The key advantage of the optimized WR algorithm over the classical WR algorithm is its faster and much more uniform convergence which can be translated into making the partitioning effort much simpler and the overall solution time faster.

It was shown in [12] that when applying the classical WR algorithm to Partial Differential Equations (PDEs), then the coupling between the sub-domains in physical space corresponds to Dirichlet transmission conditions at the interfaces introduced between sub-domains. Recent work in PDEs shows that these transmission conditions are far from optimal [13]. Importantly, it was shown that much faster convergence can be obtained if additional derivative information is exchanged in the transmission conditions. Here, we are applying the idea of improving the transmission conditions to the circuit domain.

The state of the art for the application of the classical WR algorithm to circuit problems has been summarized in a recent paper [14]. The classical WR algorithm exchanges only nodal voltage values between subsystems. Here we propose new transmission conditions which exchange a combination of voltages as well as currents. We show that the optimized WR approach leads to higher accuracy as
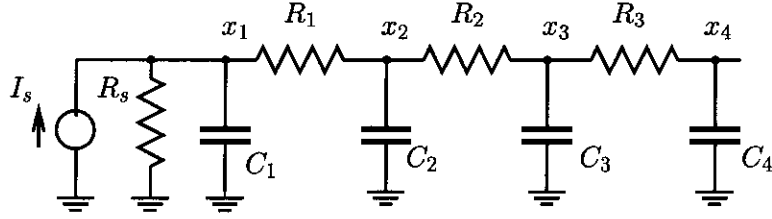
1

Figure 1: A Small example RC circuit.

well as much more uniform convergence in very few iterations. We exemplify the application of the new approach to the well known subclass of *RC* circuits. This type of circuit has been investigated for the classical WR algorithm by several authors e.g. [15, 16, 17, 18]. The small example circuit analyzed in the first part of this paper is shown in Figure 1. In the second part, we analyze the large circuit shown in Figure 10, which leads to much larger subsystem circuits, and illustrates that the size of the circuit does not have a major impact on the convergence of the optimized WR algorithm.

Nowadays, the circuit equations are usually specified in terms of the state or modified nodal analysis equations (MNA) [3], in the form $C\dot{x}(t) + Gx(t) = Bu(t)$, where C contains the reactive elements, G the other elements, while B is the input selector matrix, and $u(t)$ represents the forcing functions. For our model problems, consisting of series connected circuits only, we rewrite the MNA circuit equation into a simplified tridiagonal form

$$\dot{x} = \begin{bmatrix} b_1 & c_1 & & & \\ a_1 & b_2 & c_2 & & \\ & a_2 & b_3 & c_3 & \\ & & a_3 & b_4 & \ddots \\ & & & \ddots & \ddots \end{bmatrix} x + f. \tag{1.1}$$

The solution is sought for a given initial condition $x(0) = x^0$ and the values a_i, b_i and c_i for $i = 1, 2, \ldots$ are given by the circuit.

In Section 2 we give details for a small circuit problem and we analyze the convergence of the classical WR algorithm in Subsection 2.1. We then introduce in Subsection 2.2 the optimized WR algorithm for the small circuit problem and give a detailed convergence analysis. In Section 3 we introduce a larger circuit problem for which we investigate the convergence of both the classical and the optimized WR algorithm. Finally, in Section 4 we extend the analysis to multiple subsystems and conclusions are given in Section 5.

2 A Small RC Circuit Model Problem

In this section we analyze the classical and optimized WR algorithm for the *RC* example given in Figure 1 which is our small circuit model problem. The circuit equations are specified in the form of (1.1) as

$$\dot{x} = \begin{bmatrix} b_1 & c_1 & & \\ a_1 & b_2 & c_2 & \\ & a_2 & b_3 & c_3 \\ & & a_3 & b_4 \end{bmatrix} x + f \tag{2.1}$$

with the vector of unknown waveforms $x = (v_1, v_2, v_3, v_4)^T$ which represents a set of nodal voltage values for this RC or diffusion circuit. The entries in the tridiagonal matrix are given by

$$a_i = \frac{1}{R_i C_{i+1}}; \quad b_i = \begin{cases} -\left(\frac{1}{R_s} + \frac{1}{R_1}\right)\frac{1}{C_1} \\ -\left(\frac{1}{R_{i-1}} + \frac{1}{R_i}\right)\frac{1}{C_i}, \quad i = 2,3 \\ -\frac{1}{R_3 C_4}, \end{cases} \quad c_i = \frac{1}{R_i C_i}$$

where the resistor values R and the capacitors C are for consistency strictly positive constants. The source term on the right hand side is given by $f(t) = (I_s(t)/C_1, 0, 0, 0)^T$ for some source function $I_s(t)$ and we are also given the initial voltage values $x(0) = (v_1^0, v_2^0, v_3^0, v_4^0)^T$ at time $t = 0$.

2.1 Analysis of the Classical WR Algorithm

We partition the circuit into two sub-circuits or subsystems and we call the unknown voltages in subsystem 1 $u(t)$ and in subsystem 2 $w(t)$. Then the classical WR algorithm applied to (2.1) with two sub-circuits is given by

$$\begin{aligned}
\dot{u}^{k+1} &= \begin{bmatrix} b_1 & c_1 \\ a_1 & b_2 \end{bmatrix} u^{k+1} + \begin{pmatrix} f_1 \\ f_2 \end{pmatrix} + \begin{pmatrix} 0 \\ c_2 w_1^k \end{pmatrix} \\
\dot{w}^{k+1} &= \begin{bmatrix} b_3 & c_3 \\ a_3 & b_4 \end{bmatrix} w^{k+1} + \begin{pmatrix} f_3 \\ f_4 \end{pmatrix} + \begin{pmatrix} a_2 u_2^k \\ 0 \end{pmatrix}
\end{aligned} \tag{2.2}$$

with corresponding initial conditions $u^{k+1}(0) = (v_1^0, v_2^0)^T$ and $w^{k+1}(0) = (v_3^0, v_4^0)^T$. To start the WR iteration, we need to specify four initial waveforms $u^0(t) = (u_1^0(t), u_2^0(t))^T$ and $w^0(t) = (w_1^0(t), w_2^0(t))^T$ for $t \in [0, T]$ where T is the end of the transient analysis interval. The Laplace transform is used for the convergence study of the linear circuit considered here. It suffices to analyze the homogeneous problem where the initial conditions, $u^{k+1}(0) = w^{k+1}(0) = (0, 0)^T$, as well as source terms, $f(t) = (0, 0, 0, 0)^T$, are zero. The Laplace transform for $s \in \mathbb{C}$ of (2.2) is given by

$$s\hat{u}^{k+1} = \begin{bmatrix} b_1 & c_1 \\ a_1 & b_2 \end{bmatrix} \hat{u}^{k+1} + \begin{pmatrix} 0 \\ c_2 \hat{w}_1^k \end{pmatrix}, \quad s\hat{w}^{k+1} = \begin{bmatrix} b_3 & c_3 \\ a_3 & b_4 \end{bmatrix} \hat{w}^{k+1} + \begin{pmatrix} a_2 \hat{u}_2^k \\ 0 \end{pmatrix}. \tag{2.3}$$

Solving the first equation in (2.3) for $\hat{u}_2^{k+1}$ we find

$$\hat{u}_2^{k+1} = \frac{c_2(s - b_1)}{(s - b_1)(s - b_2) - a_1 c_1} \hat{w}_1^k \tag{2.4}$$

and similarly solving the second equation in (2.3) for $\hat{w}_1^{k+1}$ we get

$$\hat{w}_1^{k+1} = \frac{a_2(s - b_4)}{(s - b_3)(s - b_4) - a_3 c_3} \hat{u}_2^k. \tag{2.5}$$

Inserting (2.5) at iteration k into (2.4) we find a relation over two iteration steps of the WR algorithm,

$$\hat{u}_2^{k+1} = \rho_{cla}(s, a, b, c)\hat{u}_2^{k-1}$$

with the convergence rate ρ_{cla} of the classical WR algorithm given after a short computation by

$$\rho_{cla}(s, a, b, c) = \frac{c_2(s - b_1)}{(s - b_1)(s - b_2) - a_1 c_1} \cdot \frac{a_2(s - b_4)}{(s - b_3)(s - b_4) - a_3 c_3}. \tag{2.6}$$

The same result holds for $\hat{w}_1^{k+1}$ and by induction we find $\hat{u}_2^{2k} = (\rho_{cla})^k \hat{u}_2^0$ and $\hat{w}_1^{2k} = (\rho_{cla})^k \hat{w}_1^0$. For convergence we need that $|\rho_{cla}(s, a, b, c)| < 1$ for $\Re(s) > 0$ and for fast convergence the modulus of ρ_{cla}
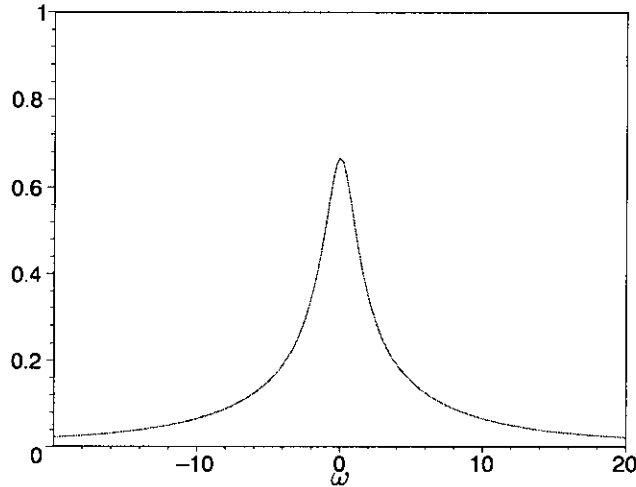
Figure 2: Convergence rate as a function of the frequency parameter ω for the classical WR algorithm applied to the small RC circuit.

should be much smaller than 1, $|\rho_{cla}| \ll 1$. But ρ_{cla} is a fixed function of the circuit parameters in the classical WR algorithm as is evident from (2.6). Thus the algorithm does not have any adjustable parameters like the optimized WR algorithm below. Hence, we can only analyze for the classical WR algorithm if the convergence test $|\rho_{cla}| < 1$ is satisfied. Checking for poles in (2.6) we find for the first quotient in ρ_{cla} that the denominator vanishes if

$$s_\pm = \frac{1}{2} \left(b_1 + b_2 \pm \sqrt{(b_1 - b_2)^2 + 4c_1 a_1} \right)$$

with a similar result for the poles of the second quotient in ρ_{cla} given in (2.6). For RC circuits, the inverse time constants are positive, $a_i, c_i > 0$, and we also have $b_1, b_2 < 0$. Hence the poles lie on the real axis, and if in addition $b_1 b_2 \geq a_1 c_1$ then they are negative, $s_\pm < 0$. A similar evaluation of the second factor shows that the poles are in the left half plane if $b_3, b_4 < 0$ and $b_3 b_4 \geq a_3 c_3$. It should be noted that this investigation is necessary since the transmission condition may introduce additional poles which are not present in the original circuit in Fig 1, for which we know that the poles are on the negative real axis.

Under the given conditions, the convergence rate ρ_{cla} is an analytic function for $s = \sigma + i\omega$ whenever $\sigma > 0$. Here ω is the angular frequency, $\omega \in \mathbb{R}$. By the maximum principle for complex analytic functions, the modulus of ρ_{cla} takes its maximum on the boundary at $\sigma = 0$, e.g. [19]. To find the location of the maximum, we separately investigate the two quotients in ρ_{cla} given in (2.6). From an explicit computation we find that they both have their maximum at $w = 0$ for the circuit at hand. Hence, the low frequencies, ω close to zero, or slow rise time aspects of the signals, converge most slowly. An example for the convergence rate as a function of ω is given in Figure 2.

In general, the classical WR algorithm for this type of problems has a smoothing property due to the low pass behavior of diffusive problems or circuits. The smoothing properties in space of classical WR algorithms for parabolic problems have been used successfully in [20, 21] for multi-grid WR algorithms. However, for a classical WR circuit solver the slow, low frequency, convergence dominates the overall convergence behavior. This aspect of the classical WR algorithm is greatly improved in the next Subsection by the optimized WR algorithm.

2.2   An Optimized WR Algorithm

The key improvements in our new WR algorithm are better transmission conditions than the ones used for the classical WR algorithm. It is natural that the WR convergence will be slow if the

4

information exchange at the interface between two subsystems is ineffective. We first recall the classical transmission conditions employed in (2.2) which can be written explicitly as

$$u_3^{k+1} = w_1^k, \quad w_0^{k+1} = u_2^k. \tag{2.7}$$

From this we see that the voltages u_3 and w_0 are directly replaced in (2.2) by voltage sources. Hence, this corresponds to exchanging voltages only at the boundaries of the partition between the two subsystems. Once the WR iteration process is converged we obtain with the classical transmission conditions

$$u_3^\infty = w_1^\infty, \quad w_0^\infty = u_2^\infty. \tag{2.8}$$

Under these conditions, the nodes at the subsystem boundaries assume the converged voltages, as expected.

For the optimized WR algorithm we propose the new, more sophisticated transmission conditions

$$(u_3^{k+1} - u_2^{k+1}) + \alpha u_3^{k+1} = (w_1^k - w_0^k) + \alpha w_1^k, \quad (w_1^{k+1} - w_0^{k+1}) + \beta w_0^{k+1} = (u_3^k - u_2^k) + \beta u_2^k. \tag{2.9}$$

As can be ascertained by comparing (2.7) with the new transmission conditions (2.9) we also exchange the voltages u_3 and w_0. However, they are multiplied with a weighting factor α while the voltage difference between the nodal voltages $(u_3 - u_2)$ insures that the currents are also taken into account in the transmission conditions since we could write the current as $\alpha^{-1}(u_3 - u_2)$ where α can be viewed as a resistor. It is evident from this that (2.9) attempts to match the interface voltages as well as the currents at the interface between the subsystems. Of course, we have to show that the new transmission conditions lead to the correct converged solution of the fundamental circuit equations. This result is given in the following lemma.

Lemma 2.1 *If the WR algorithm with the new transmission conditions (2.9) converges and if*

$$(\alpha + 1)(\beta - 1) + 1 \neq 0 \tag{2.10}$$

then the converged solution of the new WR algorithm is identical to the converged solution of the classical WR algorithm with the transmission conditions (2.7).

Proof If the algorithm with the new transmission conditions converges, then the result from (2.9) will be

$$
\begin{array}{rcrcl}
(\alpha + 1) \ (u_3^\infty - w_1^\infty) & - & (u_2^\infty - w_0^\infty) & = & 0 \\
(u_3^\infty - w_1^\infty) & + & (\beta - 1) \ (u_2^\infty - w_0^\infty) & = & 0.
\end{array}
$$

Hence, for this system to imply the classical transmission conditions the determinant needs to be different from zero, which means (2.10). ∎

For the optimized WR, the equivalent to the classical WR algorithm (2.2) is

$$
\begin{aligned}
\dot{\boldsymbol{u}}^{k+1} &= \begin{bmatrix} b_1 & c_1 \\ a_1 & b_2 + \frac{c_2}{\alpha+1} \end{bmatrix} \boldsymbol{u}^{k+1} + \begin{pmatrix} f_1 \\ f_2 \end{pmatrix} + \begin{pmatrix} 0 \\ c_2 w_1^k - \frac{c_2}{\alpha+1} w_0^k \end{pmatrix} \\
\dot{\boldsymbol{w}}^{k+1} &= \begin{bmatrix} b_3 - \frac{a_2}{\beta-1} & c_3 \\ a_3 & b_4 \end{bmatrix} \boldsymbol{w}^{k+1} + \begin{pmatrix} f_3 \\ f_4 \end{pmatrix} + \begin{pmatrix} a_2 u_2^k + \frac{a_2}{\beta-1} u_3^k. \\ 0 \end{pmatrix}
\end{aligned} \tag{2.11}
$$

where the values u_3^k and w_0^k are determined by the transmission conditions (2.9). Hence, the parameters α and β enter the WR equations. Taking the Laplace transform as we did above, we find from the circuit equation for the first subsystem, after some algebra,

$$\hat{u}_2^{k+1} = \frac{(s - b_1)c_2}{N_u}((\alpha + 1)\hat{w}_1^k - \hat{w}_0^k), \quad N_u = (\alpha + 1)(s - b_1)(s - b_2) - c_1(s - b_1) - (\alpha + 1)a_1 c_1 \tag{2.12}$$

and similarly from the circuit equation for the second subsystem

$$\hat{w}_1^{k+1} = \frac{(s-b_4)a_2}{N_w}((\beta-1)\hat{u}_2^k + \hat{u}_3^k), \quad N_w = (\beta-1)(s-b_3)(s-b_4) + a_2(s-b_4) - (\beta-1)a_3c_3. \quad (2.13)$$

Next, we would like to obtain the convergence rate for the optimized WR algorithm in closed form, similar to the result in (2.6) for the classical WR algorithm. We need to derive a relation between $\hat{u}_2^{k+1}$ and $\hat{w}_1^k$ from (2.12) and similarly a relation between $\hat{w}_1^{k+1}$ and $\hat{u}_2^k$ from (2.13). Using the transmission condition

$$(\alpha+1)\hat{u}_3^{k+1} = \hat{u}_2^{k+1} + (\alpha+1)\hat{w}_1^k - \hat{w}_0^k$$

we find together with (2.12) for the first subsystem

$$\hat{u}_3^{k+1} = \left(\frac{(s-b_1)c_2 + N_u}{(\alpha+1)(s-b_1)c_2}\right)\hat{u}_2^{k+1} \quad (2.14)$$

and similarly for the second subsystem

$$\hat{w}_0^{k+1} = \left(\frac{-(s-b_4)a_2 + N_w}{(\beta-1)(s-b_4)a_2}\right)\hat{w}_1^{k+1}. \quad (2.15)$$

Inserting (2.15) at the iteration step k into (2.12) we obtain

$$\hat{u}_2^{k+1} = \frac{(s-b_1)c_2}{N_u}\left((\alpha+1) - \left(\frac{-(s-b_4)a_2 + N_w}{(\beta-1)(s-b_4)a_2}\right)\right)\hat{w}_1^k \quad (2.16)$$

and similarly for the second subsystem

$$\hat{w}_1^{k+1} = \frac{(s-b_4)a_2}{N_w}\left((\beta-1) + \left(\frac{(s-b_1)c_2 + N_u}{(\alpha+1)(s-b_1)c_2}\right)\right)\hat{u}_2^k. \quad (2.17)$$

Finally by inserting (2.17) at iteration k into (2.16) we get a relation over two iteration steps of the optimized WR algorithm,

$$\hat{u}_2^{k+1} = \rho_{opt}(s, \boldsymbol{a}, \boldsymbol{b}, \boldsymbol{c}, \alpha, \beta)\hat{u}_2^{k-1}.$$

where the detailed convergence rate is found after replacing N_u and N_w from (2.12), (2.13)

$$\rho_{opt}(s, \boldsymbol{a}, \boldsymbol{b}, \boldsymbol{c}, \alpha, \beta) = -\frac{c_2(s-b_1)(\beta-1)+(s-b_1)(s-b_2)-a_1c_1}{((s-b_3)(s-b_4)-a_3c_3)(\beta-1)+a_2(s-b_4)} \cdot \frac{-a_2(s-b_4)(\alpha+1)+(s-b_3)(s-b_4)-a_3c_3}{((s-b_1)(s-b_2)-a_1c_1)(\alpha+1)+c_2(b_1-s)}. \quad (2.18)$$

The same result also holds for subsystem 2 and by induction we find as before $\hat{u}_2^{2k} = (\rho_{opt})^k \hat{u}_2^0$ and $\hat{w}_1^{2k} = (\rho_{opt})^k \hat{w}_1^0$. From the convergence rate (2.18) we can derive the optimal values of the parameters α and β as summarized in the following theorem.

Theorem 2.2 (Optimal Convergence) *The optimized WR algorithm (2.11) converges in two iterations if*

$$\alpha := \frac{-a_3c_3}{(s-b_4)a_2} + \frac{s-b_3}{a_2} - 1, \quad \beta := \frac{a_1c_1}{(s-b_1)c_2} - \frac{s-b_2}{c_2} + 1, \quad (2.19)$$

independently of the initial waveforms $\hat{u}^0$ and $\hat{w}^0$.

Proof The convergence rate vanishes if we insert (2.19) into ρ_{opt} given by (2.18). Hence, $\hat{u}_2^2$ and $\hat{w}_1^2$ are identically zero, independent of $\hat{u}_2^0$ and $\hat{w}_1^0$. ∎

This convergence result is optimal, because the resultant waveforms in each subsystem depend in general also on the source terms f_j in the other subsystem. Hence the minimum number of iterations needed for any WR algorithm with two subsystems to converge in general is two: a first iteration

where each subsystem incorporates the information of its source terms f_j into its waveforms and then transmits this information to the neighboring subsystems, and a second iteration to incorporate this transmitted information about f_j from the neighboring subsystems into its own waveforms. Here, we analyze a Jacobi type iteration, but the Gauss-Seidel case is similar.

We observe that the optimal choice (2.19) is not just a parameter, but the Laplace transform of a linear operator in time, since it depends on s. From the s^{-1} type frequency domain behavior, we see that it corresponds to an integral operator in time. Such an operator would be expensive to implement, it would require a convolution in the transmission condition. In this small model problem, the integral operator could be avoided by multiplying the transmission conditions by $(s - b_4)$ and $(s - b_1)$ respectively. This would lead to second degree polynomials in s which corresponds to second degree time derivatives in the transmission conditions, since a multiplication with s in the frequency domain corresponds to a time derivative. Time derivatives can be implemented at a similar cost as simple voltage values in the transmission condition, since derivatives only require local information. But we will see for the larger circuit considered below that the optimal transmission condition requires an integral operator which can not be avoided. This is true for more general circuits as well and we propose therefore an approximation of the best possible transmission condition, which applies for all types of circuits. Specifically, in this paper we choose the approximation by a constant which leads to a very practical algorithm.

2.3 Optimization of the WR Algorithm

The optimization process for the WR algorithm allows us to reduce the large $\rho_{cla}(\omega)$ of the classical WR in Figure 2 and make it more uniform so that the overall convergence is faster. Mathematically, we want $|\rho_{opt}| << 1$, which leads to the min-max problem

$$\min_{\alpha,\beta} \left(\max_{\Re(s) \geq 0} |\rho_{opt}(s, \boldsymbol{a}, \boldsymbol{b}, \boldsymbol{c}, \alpha, \beta)| \right). \tag{2.20}$$

Again if ρ_{opt} is analytic then the maximum of its modulus is attained on the boundary, $s = i\omega$, by the maximum principle. Therefore, the first step in the optimization is to ensure that the convergence rate ρ_{opt} does not have any poles in the right half plane. The conditions for analyticity, with the corresponding parameter range, are given in

Lemma 2.3 *If $b_i < 0$, $a_i, c_i > 0$, $b_1 b_2 > a_1 c_1$, $b_3 b_4 > a_3 c_3$ and*

$$\alpha > \frac{c_2 |b_1|}{b_1 b_2 - a_1 c_1} - 1 =: \underline{\alpha}, \quad \beta < -\frac{a_2 |b_4|}{b_3 b_4 - a_3 c_3} + 1 =: \overline{\beta} \tag{2.21}$$

then the convergence rate ρ_{opt} in (2.18) is an analytic function in the right half of the complex plane.

Proof We only show the proof for the first quotient in ρ_{opt} and α, since the proof for the second quotient and β is similar. The poles of the first quotient in ρ_{opt} are given by

$$s_{\pm} = \frac{(b_1 + b_2)(\alpha + 1) + c_2 \pm \sqrt{d}}{2(\alpha + 1)}, \quad d = ((b_1 + b_2)(\alpha + 1) + c_2)^2 - 4(\alpha + 1)(b_1 b_2 - a_1 c_1) + c_2 b_2.$$

If the discriminant is negative, $d < 0$, then the poles are in the left half plane, because the condition on α in (2.21) implies

$$
\begin{aligned}
(b_1 + b_2)(\alpha + 1) + c_2 &= -(|b_1| + |b_2|)(\alpha + 1) + c_2 \\
&< \frac{-(|b_1| + |b_2|)c_2 |b_1| + c_2 |b_1||b_2| - a_1 c_1 c_2}{b_1 b_2 - a_1 c_1} \\
&= \frac{-|b_1|^2 c_2 - a_1 c_1 c_2}{b_1 b_2 - a_1 c_1} < 0.
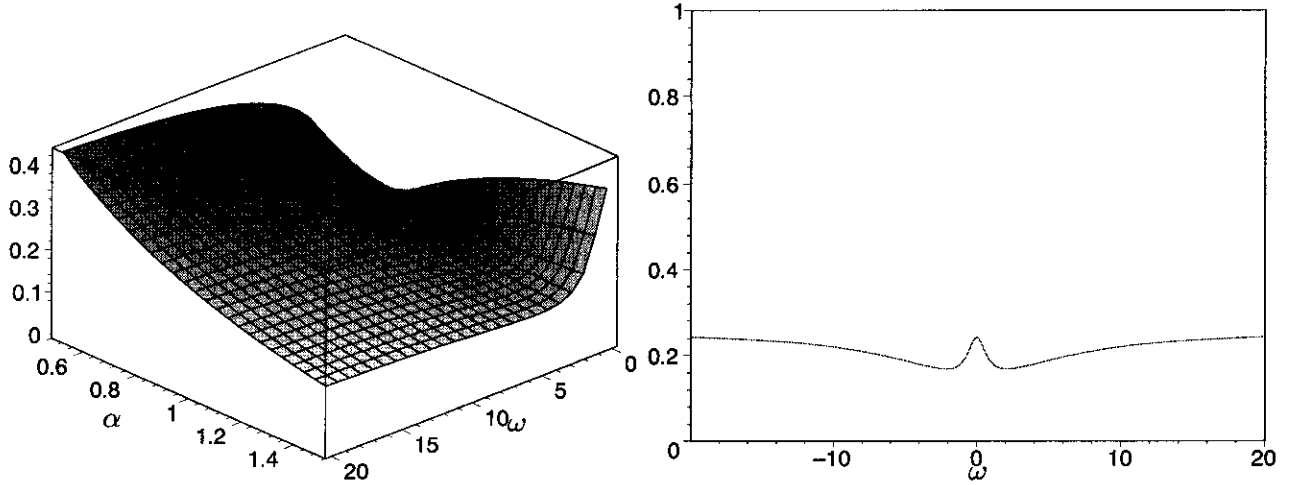\end{aligned}
$$

7

Figure 3: Left: Convergence rate $|\rho_{opt}(\alpha, \omega)|$; Right: Optimized convergence rate $|\rho_{opt}(\alpha^*, \omega)|$.

If the discriminant is positive, $d > 0$, then the poles lie on the real line and with the condition on α in (2.21) we get

$$(\alpha + 1)(b_1 b_2 - a_1 c_1) + c_2 b_2 > \frac{c_2 |b_1|}{b_1 b_2 - a_1 c_1}(b_1 b_2 - a_1 c_1) + c_2 b_2 = 0$$

which implies $\sqrt{d} < |(b_1 + b_2)(\alpha + 1) + c_2|$. Therefore, $(b_1 + b_2)(\alpha + 1) + c_2 \pm \sqrt{d} < 0$ which implies again $s_\pm < 0$. ∎

Since ρ_{opt} is analytic we can apply the maximum principle for analytic functions [19]. The maximum of $|\rho_{opt}(s)|$ for $s = \sigma + i\omega$, $\sigma > 0$ is attained on the boundary at $\sigma = 0$. The above analysis simplifies the optimization problem to

$$\min_{\alpha > \underline{\alpha}, \beta < \overline{\beta}} \left(\max_{|\omega| < \omega_{max}} |\rho_{opt}(i\omega, \boldsymbol{a}, \boldsymbol{b}, \boldsymbol{c}, \alpha, \beta)| \right) \tag{2.22}$$

where we truncated the frequency range at the largest practically relevant frequency for our problem. The maximum frequency supported by the time discretization, independent of the input waveforms, is $\omega_{max} = \pi / \Delta t$, but for practical computations often ω_{max} is considerably smaller. Additionally, one can show that the modulus of ρ_{opt} for $s = i\omega$ depends on ω^2 only, and it suffices to optimize for positive frequencies, $\omega > 0$.

To find the optimal solution of the min-max problem (2.22) in general, we need to resort to numerical methods. In our case we know that the subsystems or subcircuits have very similar electrical properties on both sides of the partitioning boundary as can be observed from Fig. 1. Further, in the next Section 2.4 we will give the circuit element values which are the same for all internal circuit elements to keep the optimization simpler. Hence, we choose $\beta = -\alpha$ where α is the single optimization parameter. We show on the left hand side of Fig. 3 $|\rho_{opt}(\alpha, \omega)|$ the result of the optimization with respect to α. We can observe that the solution of the min-max problem occurs when the convergence rate at $\omega = 0$ and at $\omega = \omega_{max}$ are balanced. Therefore, we use the equation

$$|\rho_{opt}(\alpha^*, 0)| = |\rho_{opt}(\alpha^*, \omega_{max})|$$

to determine the optimal parameter α^*. In this example if we choose $\omega_{max} = \infty$ we find $\alpha^* = 1$ and from the symmetry assumption above we obtain $\beta^* = -1$. Finally, this leads to the convergence rate shown on the right hand side in Figure 3. We see a considerable improvement in magnitude
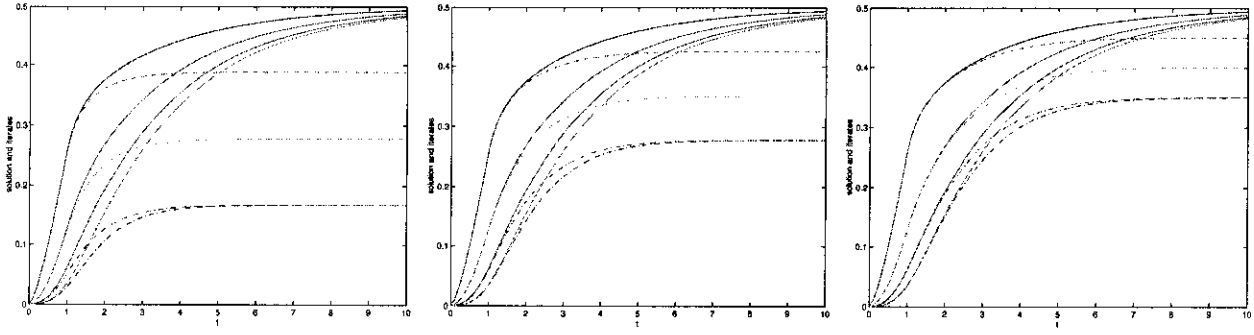
Figure 4: Iteration waveforms for classical WR. Left: iteration 3; Middle: iteration 5; Right: iteration 7
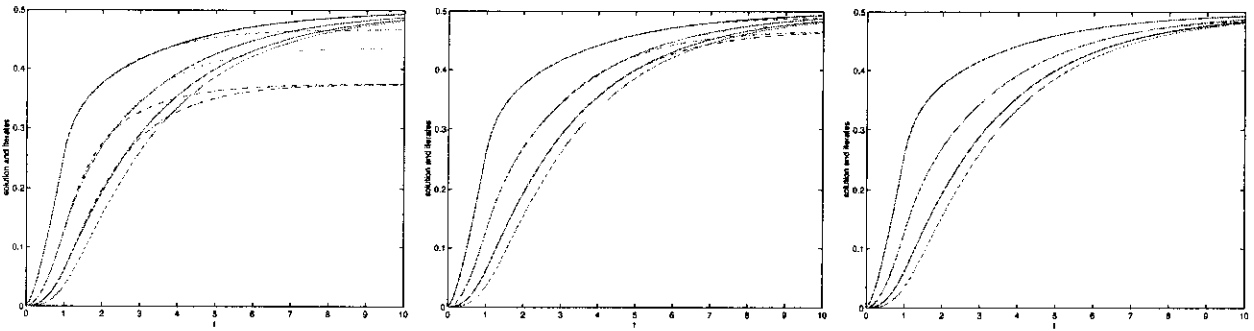

Figure 5: Iteration waveforms for optimized WR; Left: iteration 3. Middle: iteration 5; Right: iteration 7

and uniformity for the convergence rate in comparison to the classical WR method in Figure 2. The classical convergence rate has a maximum of $2/3$ at $\omega = 0$ while the optimized convergence rate has a maximum of only $1/4$ in this example.

2.4 Numerical Experiments for the Small Circuit

We next give a numerical example to illustrate the improvements in the convergence of the optimized WR algorithm over the classical one. We assume the specific typical circuit parameters

$$R_s = \frac{1}{2}, \quad R_1 = \frac{1}{2}, \ R_2 = \frac{1}{2}, \ R_3 = \frac{1}{2}, \quad C_1 = \frac{63}{100}, \ C_2 = \frac{63}{100}, \ C_3 = \frac{63}{100}, \ C_4 = \frac{63}{100}.$$

for the circuit in Figure 1. We chose for all the numerical computations the backward Euler method with a time step of $\Delta t = 1/10$. We first give the results for the classical WR in Figure 4. As a reference we show in *all* the waveform graphs the four converged waveforms at nodes 1 to 4 with the solid lines. Obviously, the highest solid voltage waveform corresponds to node 1. All the waveform graphs show (left to right) the dashed voltages for WR iterations 3, 5 and 7. The highly non-uniform convergence behavior of the classical WR is evident and the *rapid convergence* behavior early in the time interval with the very slow convergence later on in the time interval is clearly visible. Hence, good convergence behavior can only be achieved for very small windows in time [16]. However, this severely limits the efficiency of the overall approach since it leads to the mandatory introduction of small windows in time. Figure 5 shows the third, fifth and seventh iteration of the optimized WR algorithm together with the exact solution. Clearly, the convergence towards the end of the time interval, corresponding to low frequencies ω, is greatly accelerated. It is evident that the optimized WR algorithm performs much better for low frequencies since the optimized WR algorithm greatly
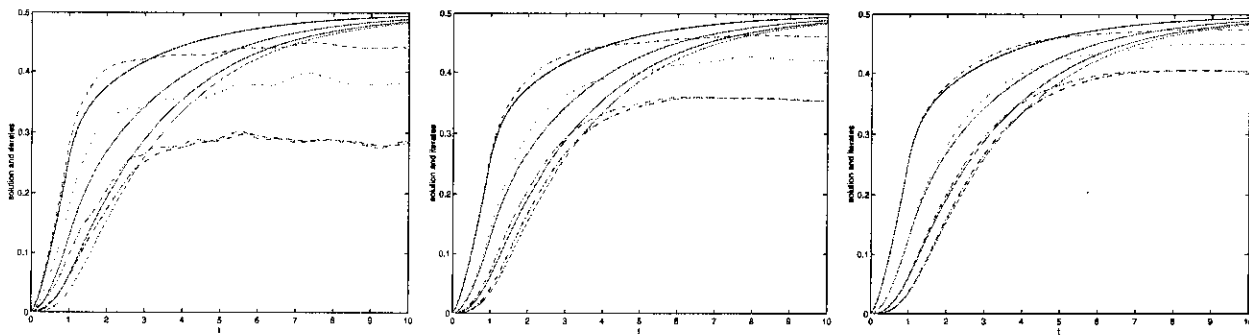
Figure 6: Iteration waveforms for classical WR. Left: iteration 3; Middle: iteration 5; Right: iteration 7
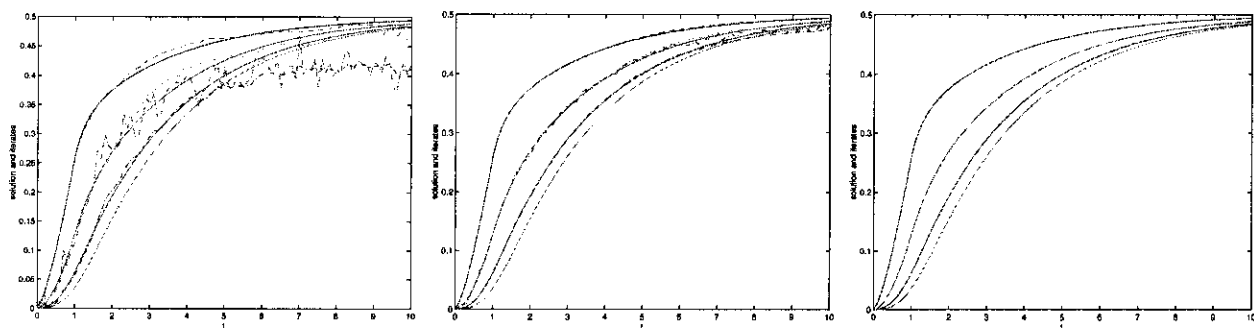

Figure 7: Iteration waveforms for optimized WR; Left: iteration 3. Middle: iteration 5; Right: iteration 7

reduces $|\rho_{opt}(0)|$. We started with zero initial waveforms and used an input step function with an amplitude of $I_s = 1$ and a rise time of 1 time unit.

We used the above wide-band frequency process which optimizes over all ω and led to $\alpha^* = -\beta^* = 1$, even though in this application low frequencies dominate, the solutions and iterates are smooth. To simulate the case of a broader frequency range, we start the WR iteration with random initial waveforms at all nodes in the circuit in Figure 1. This way we can also study the smoothing properties of the iteration process. The waveforms for this case are shown in Figure 6 for classical WR. From these Figures one can see how the classical WR algorithm exhibits smoothing properties but the convergence is slow. This is different for the optimized WR algorithm, as the sequence of images shows in Figure 7.

To contrast the difference in convergence between the two WR algorithms we finally show the error as a function of the iteration in Figure 8. The remarkable improvement of the optimized WR algorithm over the classical one is evident from this comparison.

As the last part of these numerical experiments we investigate how close the theoretically optimized parameters from Subsection 2.2 are to the parameters that perform best in our numerical experiments. In Figure 9 we varied α and β and computed the error after 20 iterations of the optimized WR. We can see that the simple optimization of equilibrating the convergence rate at frequency $\omega = 0$ and for $\omega \longrightarrow \infty$ leads to parameters which are close to the optimal numerical ones. The theoretical value (α^*, β^*) is indicated by an asterisk while the numerically optimal value is located somewhere in the 10^{-9} island nearby.
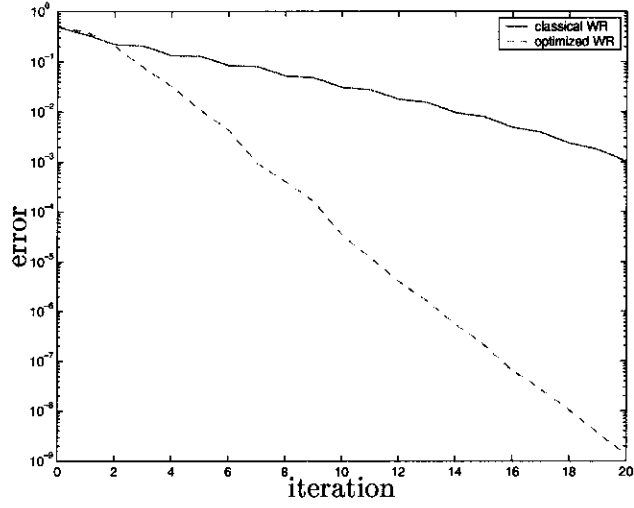
Figure 8: Convergence rates of classical versus optimized waveform relaxation.
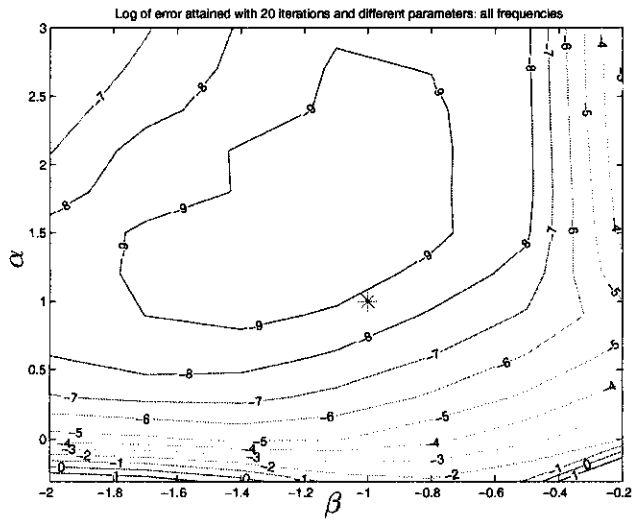

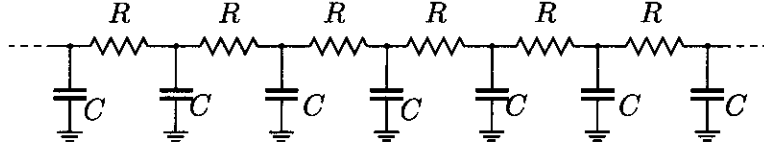Figure 9: Numerical and analytical optima compared after 20 WR iterations

Figure 10: An infinitely long RC circuit chain

3   Analysis of a Large RC Circuit

So far we have concentrated on the analysis of the relatively small circuit in Figure 1. In this Section, we investigate the impact of the circuit size on the performance of the optimized WR algorithm. In fact, in the analysis below we take the limiting case where the number of sections, or the subsystem size, is infinite as is indicated in Figure 10. This will show what the impact of the subsystem size is on the convergence properties of the algorithm. The equations for the infinitely large circuit matrix are

$$\dot{x} = \begin{bmatrix} \ddots & \ddots & \ddots & & \\ & a & b & c & \\ & & a & b & c \\ & & & \ddots & \ddots & \ddots \end{bmatrix} x + f. \tag{3.1}$$

The vector of unknown waveforms is $x = (\dots, v_{-1}, v_0, v_1, \dots)^T$ and represents an infinite set of nodal voltages. The constant entries in the tridiagonal matrix are given by

$$a = \frac{1}{RC}; \quad b = -\left(\frac{1}{2R}\right)\frac{1}{C}; \quad c = \frac{1}{RC} = a$$

where the circuit elements, R and C are assumed to be strictly positive and constant. The source term on the right hand side is given by the vector of functions $f(t) = (\dots, f_{-1}(t), f_0(t), f_1(t), \dots)^T$ and we need an initial condition $x(0) = (\dots, v_{-1}^0, v_0^0, v_1^0, \dots)^T$. Since the circuit is infinitely large, we have to assume that all voltage values stay bounded as we move towards the infinite ends of the circuit to have a well posed problem.

3.1   The Classical WR Algorithm for the Large Circuit

We formulate a block partitioned version equivalent to (2.2) of the classical WR algorithm for the circuit in Figure 10 with two sub-circuits,

$$\begin{aligned} \dot{u}^{k+1} &= \begin{bmatrix} \ddots & \ddots & \ddots & & \\ & a & b & a & \\ & & a & b & \\ b & a & & & \\ a & b & a & & \\ & \ddots & \ddots & \ddots & \end{bmatrix} \begin{matrix} u^{k+1} + \\ \\ w^{k+1} + \end{matrix} \begin{pmatrix} \vdots \\ f_{-1} \\ f_0 \\ f_1 \\ f_2 \\ \vdots \end{pmatrix} + \begin{pmatrix} \vdots \\ 0 \\ aw_1^k \\ au_0^k \\ 0 \\ \vdots \end{pmatrix} \\ \dot{w}^{k+1} &= \end{aligned} \tag{3.2}$$

with the initial conditions $u^{k+1}(0) = (\dots, v_{-1}^0, v_0^0)^T$ and $w^{k+1}(0) = (v_1^0, v_2^0, \dots)^T$. To start the WR iteration, some initial waveforms $u^0(t)$ and $w^0(t)$ are used.

As in Subsection (2.1) it suffices to analyze the homogeneous problem, $f(t) = 0$ with zero initial conditions $x(0) = 0$ for the convergence study. The Laplace transform yields in the $s \in \mathbb{C}$ domain

$$s\hat{u}^{k+1} = \begin{bmatrix} \ddots & \ddots & \ddots & \\ & a & b & a \\ & & a & b \end{bmatrix} \hat{u}^{k+1} + \begin{pmatrix} \vdots \\ 0 \\ a\hat{w}_1^k \end{pmatrix}, \quad s\hat{w}^{k+1} = \begin{bmatrix} b & a & & \\ a & b & a & \\ & \ddots & \ddots & \ddots \end{bmatrix} \hat{w}^{k+1} + \begin{pmatrix} a\hat{u}_0^k \\ 0 \\ \vdots \end{pmatrix}. \tag{3.3}$$

Solving the first system of equations for $\hat{u}_j^{k+1}$ corresponds to solving the recurrence relation

$$a\hat{u}_{j-1}^{k+1} + (b-s)\hat{u}_j^{k+1} + a\hat{u}_{j+1}^{k+1} = 0, \quad j = 0, -1, -2, \ldots$$

with the general solution

$$\hat{u}_j^{k+1} = A^{k+1}\lambda_+^j + B^{k+1}\lambda_-^j$$

where $\lambda_\pm$ are the roots of the characteristic polynomial of the recurrence relation,

$$\lambda_\pm = \frac{s - b \pm \sqrt{(s-b)^2 - 4a^2}}{2a}. \tag{3.4}$$

To determine the constants A^{k+1} and B^{k+1} for the general solution, we need to use the transmission condition at the subsystem interface and the boundedness condition at infinity. Some algebra shows that for $|b| \geq 2a$ and $s = \sigma + i\omega$ with $\sigma > 0$ we have $|\lambda_+| > 1$ and $|\lambda_-| < 1$ and by the boundedness condition we obtain $B^{k+1} = 0$. Further, we can determine A^{k+1} from the last equation at the interface,

$$a\hat{u}_{-1}^{k+1} + (b-s)\hat{u}_0^{k+1} = A^{k+1}(a\lambda_+^{-1} + b - s) = -a\hat{w}_1^k$$

which leads to

$$A^{k+1} = -\frac{a\hat{w}_1^k}{(a\lambda_+^{-1} + b - s)}.$$

Hence the general solution for $\hat{u}_j^{k+1}$ is given by

$$\hat{u}_j^{k+1} = -\frac{a\hat{w}_1^k}{(a\lambda_+^{-1} + b - s)}\lambda_+^j. \quad j = 0, -1, -2, \ldots \tag{3.5}$$

Similarly, solving the second subsystem for $\hat{w}_j^{k+1}$ we obtain

$$\hat{w}_j^{k+1} = -\frac{a\hat{u}_0^k}{a\lambda_- + b - s}\lambda_-^{j-1}, \quad j = 1, 2, 3, \ldots \tag{3.6}$$

Inserting this result at iteration k into (3.5) we find over two iteration steps the mapping

$$\hat{u}_0^{k+1} = \rho_{cla}(s, a, b)\hat{u}_0^{k-1}$$

where the convergence rate ρ_{cla} is given by

$$\rho_{cla}(s, a, b) = \frac{a^2}{(a\lambda_+^{-1} + b - s)(a\lambda_- + b - s)} = \frac{1}{\lambda_+^2}. \tag{3.7}$$

To obtain the last equality on the right, we used the formula for $\lambda_\pm$ given in (3.4). Since the same result holds for $\hat{w}_1^{k+1}$ we find by induction as usual $\hat{u}_0^{2k} = (\rho_{cla})^k \hat{u}_0^0$ and $\hat{w}_1^{2k} = (\rho_{cla})^k \hat{w}_1^0$. Hence, for a large number of iterations the classical WR always converges, since $|\lambda_+| > 1$. Also, the convergence rate is analytic for $s = \sigma + i\omega$ with $\sigma > 0$ under the condition $2a \leq |b|$. We again use the maximum principle for analytic functions [19] to find the maximum of $|\rho_{cla}|$ to be on the boundary of the right half of the complex plane, at $\sigma = 0$. However, taking the limit on the boundary as ω goes to zero, we find that

$$|\rho_{cla}| = \frac{|b| - \sqrt{b^2 - 4a^2}}{|b| + \sqrt{b^2 - 4a^2}} = 1 \text{ if } 2a = |b|.$$

Unfortunately, often for RC type circuits, or diffusion type equations in general, the last equality is satisfied. This implies that convergence will be very slow for low frequencies ω close to zero and the mode $\omega = 0$ will not converge. Fortunately, in a realistic transient analysis, the frequency $\omega = 0$ can
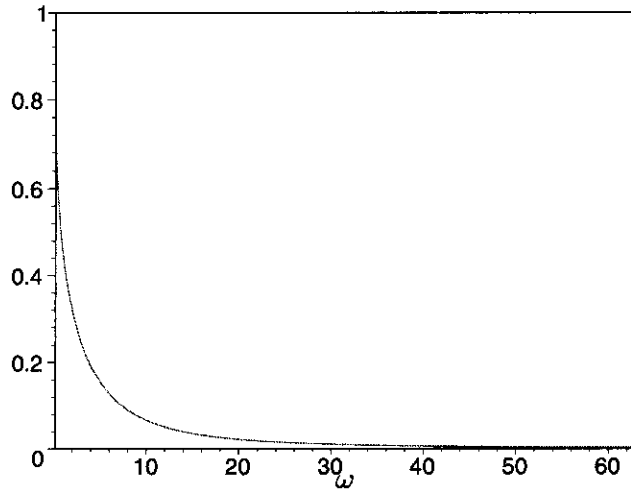
Figure 11: Convergence rate as a function of the frequency parameter ω for WR applied to the large RC circuit with a lower bound on the frequencies, $|\omega| > \omega_{\min}$.

not appear in the error, because the error at $t = 0$ is zero, since the initial condition is known. The estimate for the lowest frequency occurring in the transient analysis depends on the length of the time interval $[0, T]$. We expand the signal in a Fourier series $\sin(k\pi t/T)$ for $k = 1, 2, \ldots$. This leads to the estimate $\omega_{\min} = \pi/T$ for the lowest relevant frequency. If, for example, the transient analysis time is $T = 20$, we get $\omega_{\min} = \pi/20$. The highest frequency $\omega_{\max}$ depends again on the resolution of the discretization in time, and we use as before $\omega_{\max} = \pi/\Delta t$ which is the highest possible oscillation on a grid with spacing Δt.

In our numerical experiments for the large system we use a system with 100 nodes total and a transient analysis time $T = 20$ with a time step $\Delta t = 1/20$. The circuit elements are the same as those used in the numerical experiments for the small circuit in Subsection 3.4. For this example the dependence of the convergence rate on ω is given in Figure 11 for positive ω's only due to symmetry. By comparing the convergence rate for the small subsystem example in Figure 2 we observe that the convergence behavior is very similar, low frequencies converge slowly and high frequencies converge very fast.

3.2 The Optimal WR Algorithm for the Large Circuit

To obtain an optimized WR algorithm, we replace similarly to the small circuit case the classical transmission conditions

$$u_1^{k+1} \equiv w_1^k, \quad w_0^{k+1} \equiv u_0^k$$

by the new transmission conditions given in (2.9),

$$(u_1^{k+1} - u_0^{k+1}) + \alpha u_1^{k+1} = (w_1^k - w_0^k) + \alpha w_1^k, \quad (w_1^{k+1} - w_0^{k+1}) + \beta w_0^{k+1} = (u_1^k - u_0^k) + \beta u_0^k. \quad (3.8)$$

Analogous to the small RC circuit case, these new transmission conditions imply the old ones at convergence by Lemma 2.1. The partitioned infinite system with the parameters α and β for the

optimized WR is given by

$$
\begin{aligned}
\dot{u}^{k+1} &= \begin{bmatrix} \ddots & \ddots & \ddots & & \\ & a & b & a & \\ & & a & b+\frac{a}{\alpha+1} \end{bmatrix} u^{k+1} + \begin{pmatrix} \vdots \\ f_{-1} \\ f_0 \end{pmatrix} + \begin{pmatrix} \vdots \\ 0 \\ aw_1^k - \frac{a}{\alpha+1}w_0^k \end{pmatrix} \\
\dot{w}^{k+1} &= \begin{bmatrix} b-\frac{a}{\beta-1} & a & \\ a & b & a \\ & \ddots & \ddots & \ddots \end{bmatrix} w^{k+1} + \begin{pmatrix} f_1 \\ f_2 \\ \vdots \end{pmatrix} + \begin{pmatrix} au_0^k + \frac{a}{\beta-1}u_1^k \\ 0 \\ \vdots \end{pmatrix}
\end{aligned}
\tag{3.9}
$$

together with the transmission conditions (3.8) which define the values u_1^k and w_0^k. Taking the Laplace transform $s \in \mathbb{C}$ as before and assuming that solutions stay bounded, we find the same type solution for the recurrence relation as in the classical WR algorithm,

$$
\hat{u}_j^{k+1} = A^{k+1}\lambda_+^j, \ j=1,0,-1,-2,\dots \qquad \hat{w}_j^{k+1} = B^{k+1}\lambda_-^{j-1}, \ j=0,1,2,3,\dots
$$

where the constants A^{k+1} and B^{k+1} are now different due to the new transmission conditions. Using (3.8) we find

$$
A^{k+1} = \frac{(\alpha+1)-\lambda_-^{-1}}{(\alpha+1)\lambda_+ - 1}B^k, \quad B^{k+1} = \frac{(\beta-1)+\lambda_+}{(\beta-1)\lambda_-^{-1}+1}A^k.
$$

Applying the second relation at step k to the first one, we find

$$
\hat{u}_0^{k+1} = \rho_{opt}(s,a,b,\alpha,\beta)\hat{u}_0^{k-1}
$$

where the convergence rate ρ_{opt}, using that $\lambda_+ = 1/\lambda_-$, is given by

$$
\rho_{opt}(s,a,b,\alpha,\beta) = \frac{(\alpha+1)-\lambda_+}{(\alpha+1)\lambda_+-1} \cdot \frac{(\beta-1)+\lambda_+}{(\beta-1)\lambda_++1}
\tag{3.10}
$$

The same relation also holds for the other subsystem and by induction we find $\hat{u}_0^{2k} = (\rho_{opt})^k\,\hat{u}_0^0$ and $\hat{w}_1^{2k} = (\rho_{opt})^k\,\hat{w}_1^0$.

Theorem 3.1 (Optimal Convergence) *The optimized WR algorithm (2.11) converges in two iterations for the choice of parameters*

$$
\hat{\alpha} := \lambda_+ - 1, \quad \hat{\beta} := -\lambda_+ + 1
\tag{3.11}
$$

independently of the guess for the initial waveforms.

Proof The proof is similar to the small circuit case in Subsection 2.2. ∎

3.3 Optimization Process for the Large Circuit

The fundamental optimization process is clearly the same for the large circuit as it is for the small one. Hence, we use the min-max criterion in (2.20) and the same fundamental overall approach to get the best performance of the new WR algorithm. Equivalent to Lemma 2.3 we have

Lemma 3.2 *The convergence rate ρ_{opt} in (3.10) is under the conditions*

$$
b < 0, \quad a > 0, \quad 2a \leq -b
\tag{3.12}
$$

$$
\alpha > 0, \quad \beta < 0
\tag{3.13}
$$

an analytic function in the right half of the complex plane, $s = \sigma + i\omega$ with $\sigma > 0$.
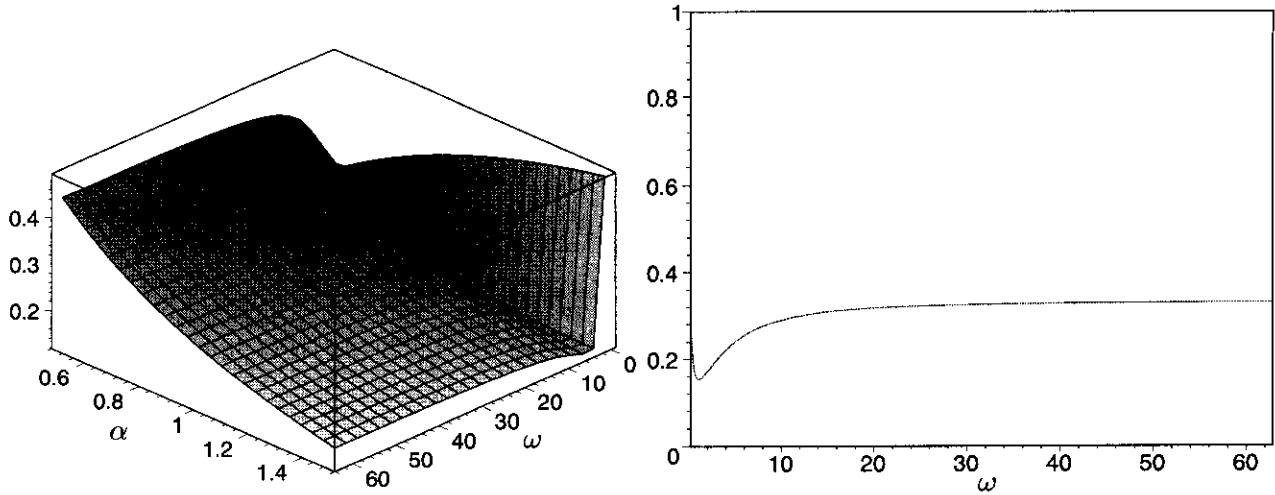
Figure 12: Left: Convergence rate $|\rho_{opt}(\alpha,\omega)|$; Right: Optimized rate $|\rho_{opt}(\alpha^*,\omega)|$.

Proof λ_+ is an analytic function in the right half plane, since the argument under the square root avoids the negative real axis under the conditions (3.12). Hence, it suffices to show that the denominator does not have zeros. But with condition (3.13) and the knowledge that $|\lambda_+| > 1$ poles are excluded. ∎

We again use the maximum principle to find the maximum in $|\rho_{opt}(s)|$ for $s = \sigma + i\omega$, $\sigma > 0$ on the boundary at $\sigma = 0$. This yields the optimization problem

$$\min_{\alpha>0, \beta<0}\left(\max_{\omega_{\min}<|\omega|<\omega_{\max}} |\rho_{opt}(i\omega, a, b, \alpha, \beta)|\right)$$

where we truncated the frequency range by a minimal and maximal frequency relevant for our problem as we did earlier. We again use the similarity of the subsystems as was done above in Section 2.3 for the small circuits. The subsystems in the large circuit are behaving identically on both sides of the partition, so we again assume for simplicity that $\beta = -\alpha$, although this may not give the best possible solution. This assumption simplifies the optimization process and leads for the numerical example in Subsection 3.4 to the surface for $|\rho_{opt}(\alpha,\omega)|$ given in Figure 12 on the left. There we can see that the solution of the min-max problem is obtained when the convergence rate at $\omega = \omega_{\min}$ and the convergence rate at $\omega = \omega_{\max}$ are balanced, which gives the equation

$$|\rho_{opt}(\alpha^*, \omega_{\min})| = |\rho_{opt}(\alpha^*, \omega_{\max})|$$

to be solved for the optimal parameter α^*. For the example with $\omega_{\min} = \pi/T$ and $\omega_{\max} = \pi/\Delta t$ we find $\alpha^* = 0.73455$ which leads to the convergence rate shown in Figure 12 on the right. The maximum is about 0.33 and should be compared with the rate obtained by the classical WR with maximum 0.73, shown in Figure 11.

3.4 Numerical Experiments for the Large Circuit

We solve a model circuit with 100 nodes with the same fundamental parameters as we did for the small circuit,

$$R_s = \frac{1}{2}, \quad R_i = \frac{1}{2}, \ i = 1,\ldots,99 \quad C_i = \frac{63}{100}, \ i = 1,\ldots,100.$$

The solution approach is again based on the backward Euler integration technique and our transient analysis time is $t \in [0, 20]$ with a time step of $\Delta t = 1/20$. From this we find the error as a function of the WR iterations where we use a random initial starting waveform to get a distributed spectrum.
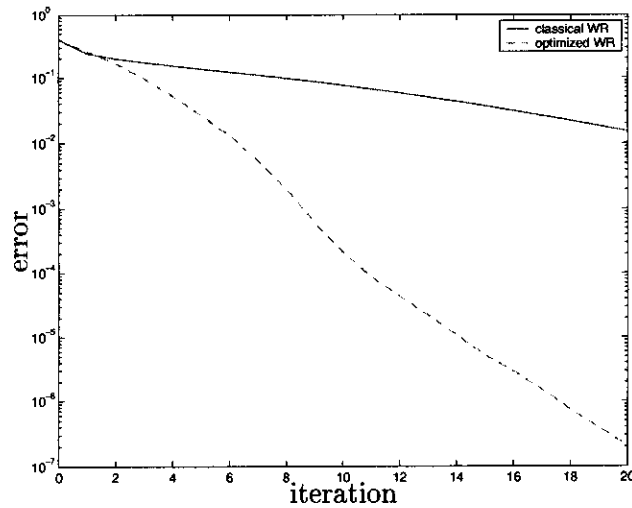
16

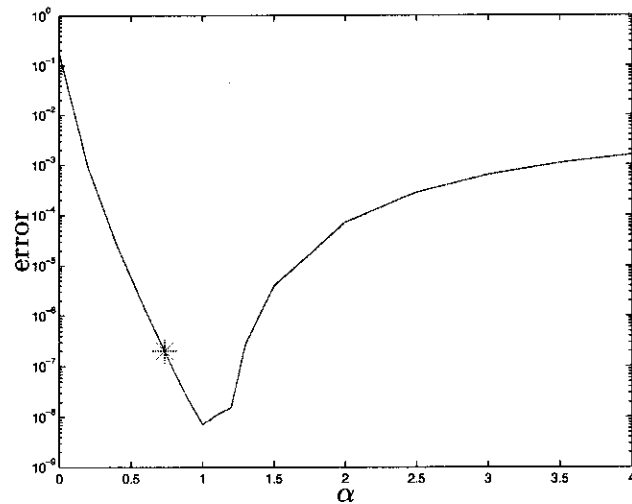Figure 13: Convergence rates of classical versus optimized WR.

Figure 14: Numerical and analytical optima compared.

The result for the optimized WR algorithm in Figure 13 show how strongly the convergence rate has been improved by the optimization process compared to the classical WR algorithm. One can also compare the result for the large subsystems with the error decay for the small subsystems in Figure 8 which shows that the convergence for both the classical and the optimized WR algorithms is similar, in spite of the large difference in the subsystem size.

We finally investigated how close the theoretically optimal parameter α^* is to the best possible one for the numerical code. In Figure 14 we varied α and computed the error after 20 iterations of the optimized WR algorithm. Again the simple optimization of equilibrating the convergence rate at the lowest frequency $\omega_{\min}$ and highest frequency $\omega_{\max}$ leads to parameters which are close to the optimal numerical ones as shown in Figure 14.

4 Multiple Subsystems

So far we investigated the local convergence of the optimized WR algorithm between two subsystems. In real life applications the circuit needs to be partitioned into multiple subsystems to gain a speedup advantage over a flat single matrix analysis. In this Section we investigate the impact of multiple

17

subsystems on the convergence for the optimized WR algorithm. We work again with the large circuit given in Figure 10. The circuit is partitioned into N subsystems with corresponding solutions $\boldsymbol{u}_n$, $n = 1, 2, \ldots N$, and we assume that each subsystem has the number of nodal voltage values M_n. The optimized waveform relaxation algorithm then becomes

$$
\begin{aligned}
\dot{\boldsymbol{u}}_1^{k+1} &= \begin{bmatrix} \ddots & \ddots & \ddots \\ & a & b & a \\ & & a & b + \frac{a}{\alpha+1} \end{bmatrix} \boldsymbol{u}_1^{k+1} + \begin{pmatrix} \vdots \\ 0 \\ au_{2,2}^k - \frac{a}{\alpha+1}u_{2,1}^k \end{pmatrix} \\
\dot{\boldsymbol{u}}_n^{k+1} &= \begin{bmatrix} b - \frac{a}{\beta-1} & a \\ a & b & a \\ & \ddots & \ddots & \ddots \\ & & a & b & a \\ & & & a & b + \frac{a}{\alpha+1} \end{bmatrix} \boldsymbol{u}_n^{k+1} + \begin{pmatrix} au_{n-1,J_{n-1}-1}^k + \frac{a}{\beta-1}u_{n-1,J_{n-1}}^k \\ 0 \\ \vdots \\ 0 \\ au_{n+1,2}^k - \frac{a}{\alpha+1}u_{n+1,1}^k \end{pmatrix}, \ n = 2, 3 \ldots N - 1 \\
\dot{\boldsymbol{u}}_N^{k+1} &= \begin{bmatrix} b - \frac{a}{\beta-1} & a \\ a & b & a \\ & \ddots & \ddots & \ddots \end{bmatrix} \boldsymbol{u}_N^{k+1} + \begin{pmatrix} au_{N-1,J_{N-1}-1}^k + \frac{a}{\beta-1}u_{N-1,J_{N-1}}^k \\ 0 \\ \vdots \end{pmatrix}
\end{aligned}
$$

$$(4.1)$$

where n represents the subsystem number.

Note that we have not included a source term $\boldsymbol{f}$ in (4.1), because by linearity it suffices to analyze the homogeneous system as before. We will consider a more typical case below, with a small number of sources, after considering first the general result where each subsystem can have its own source.

Theorem 4.1 (Convergence in N iterations) *If the optimal transmission conditions from (3.11) are used, $\alpha := \lambda_+ - 1$ and $\beta := -\lambda_+ + 1$, then the optimized WR algorithm (4.1) converges in N iterations.*

Proof Laplace-transforming each subsystem, we find the general solution on subsystem n like in the case of two subsystems to be

$$
\hat{u}_{n,j}^{k+1} = A_n^{k+1}\lambda_+^j + B_n^{k+1}\lambda_-^j, \quad n = 1, 2, \ldots N. \tag{4.2}
$$

In the first iteration we find on the first subsystem the constant $B_1^1 = 0$, because the solution stays bounded at infinity, and the first iterate on the first subsystem is $\hat{u}_{1,j}^1 = A_1^1\lambda_+^j$. This solution is now used in the second iteration by the second subsystem in the transmission condition, and we find

$$
a\hat{u}_{1,J_1-1}^1 + \frac{a}{\beta-1}\hat{u}_{1,J_1}^1 = aA_1^1\lambda_+^{J_1-1}\left(1 + \frac{1}{\beta-1}\lambda_+\right) = 0
$$

because of the special choice of β. Hence, a zero transmission condition is imposed on the second subsystem on the left in the second iteration,

$$
\hat{u}_{2,1}^2\left(s - \left(b - \frac{a}{\beta-1}\right)\right) - a\hat{u}_{2,2}^2 = 0.
$$

Inserting the general form (4.2) of the solution into this transmission condition, we obtain, using $\beta = -\lambda_+ + 1$ and $\lambda_+\lambda_- = 1$

$$
\begin{aligned}
(A_2^2\lambda_+ + B_2^2\lambda_-)&\left(s - \left(b - \frac{a}{\beta-1}\right)\right) - a(A_2^2\lambda_+^2 + B_2^2\lambda_-^2) \\
&= A_2^2(\lambda_+(s - b) - a - a\lambda_+^2) + B_2^2(\lambda_-(s - (b + a/\lambda_+)) - a\lambda_-^2) \\
&= -A_2^2(a\lambda_+^2 + (b - s)\lambda_+ + a) - B_2^2\lambda_-((b - s) + 2a\lambda_-) \quad = \quad 0.
\end{aligned}
$$

Now, the factor multiplying A_2^2 vanishes identically, since λ_+ is exactly a root of the quadratic equation. Since the factor multiplying B_2^2 does not vanish, we must have $B_2^2 = 0$ and the second iterate

18

on the second sub-circuit is again of the form $\hat{u}_{2,j}^2 = A_2^2 \lambda_+^j$ as the first iterate was on the first sub-system. By induction at iteration N we have $B_n^N = 0$ for all $n = 1, 2, \ldots N$. A similar argument can be applied in the other direction for the coefficients A_n^k and we find at iteration N that $A_n^N = 0$ for all $n = 1, 2, \ldots N$ as well. Hence we have $\hat{u}_{n,j}^N = 0$ for all waveforms and the algorithm has converged. ∎

It is important to note that this is again an optimal result. No other WR algorithm can converge faster for the case of N sequential subsystems, where each system has a source associated with it. The reason is that the solution for the last subsystem depends on the source terms in the first subsystem and vice versa. If information is exchanged only between neighboring subsystems, as is the case for classical Jacobi WR, then it can propagate at most by one subsystem for each iteration. Hence, there are at least N iterations needed to propagate the information across N sequential subsystems. The proof for a similar result for steady convection diffusion problems can be found in [22] and for the wave equation in [23].

However, for circuit applications, where the sources are usually limited to a few subsystems, an appropriate scheduling algorithm can be used which starts at the sources. In this case convergence is obtained in a few iteration with the optimal transmission conditions (3.11) if for example a *basic schedule* [10] is used. The subsystems at the sources are solved first and the other subsystems are solved in sequence in a Gauss-Seidel WR fashion. For a simple chain circuit with the source at the input e.g. Figure 1, the source term is at the leftmost subsystem. We start by solving this subsystem first. It is important to observe that we immediately find the exact solution for the optimized WR with conditions (3.11) since all the other sources in the other subsystems are zero. Finally, all the other subsystems are solved sequentially according to the schedule. This leads to the exact solution for each subsystem. Hence, we observe that the optimal transmission conditions transform the RC circuit into a quasi *one-way* circuit [10]. In general, very few practical circuits have one-way properties. An example is a chain of N ideal inverters without feeback capacitances. Of course, this circuit can be solved in one iteration with a Gauss-Seidel scheme for both the classical and the optimized algorithms.

Finally, we would like to point out that the best possible transmission conditions for the optimized WR algorithm with $N > 2$ subsystems are the same as the best transmission conditions for the WR algorithm with two subsystems. The optimal transmission conditions require an expensive time domain integral operator. To circumvent this problem, we propose to use the same optimization introduced for the two sub-circuit case in Section 3.3 for practical applications. As we have shown, the convergence is very fast for this approach.

5 Conclusions

We have shown that the convergence of the classical waveform relaxation algorithm can be drastically enhanced by improving the data exchange between the partitioned subsystems. The new concept is to exchange both voltage and current, or derivatives, rather than just voltage which was the principle behind classical waveform relation. With these new exchange quantities, which we term transmission conditions, we demonstrate rigorously that very uniform convergence can be achieved with very few iterations for RC circuits which are well known to lead to much slower, non-uniform convergence for classical waveform relaxation. This approach also makes the usually difficult partitioning process simpler since more agressive partitioning strategies can be used. The computer experiments given confirm the theoretical results.

References

[1] E. Lelarasmee, A. E. Ruehli and A. L. Sangiovanni-Vincentelli. The waveform relaxation method for time-domain analysis of large-scale integrated circuits. *IEEE Trans. on CAD of Integrated*

Circuits and Systems, CAD-1(3):131–145, July 1982.

[2] W. T. Weeks, A. J. Jimenez, G. W. Mahoney, D. Mehta, H. Quassemzadeh, and T. R. Scott. Algorithms for ASTAP - a network analysis program. *IEEE Trans. on Circuit Theory*, CT(20):628–634, November 1973.

[3] C. Ho, A. Ruehli, P. Brennan. The modified nodal approach to network analysis. *IEEE Transactions on Circuits and Systems*, pages 504–509, June 1975.

[4] L. W. Nagel. SPICE2, a computer program to simulate semiconductor circuits. Memo UCB/ERL M520, University of California, Berkeley, May 1975.

[5] J. White, A. Sangiovanni-Vincentelli. Relax 2.1 - a waveform relaxation based circuit simulation program. In *Proc. Int. Custom Integr. Circ. Conf.*, June 1984.

[6] B. Ingenbleek, B. Klassen, K-L Papp. Sisal: Ein programm zur transientenanalyse integrierter mos-schaltungen. In *GMD-Studie Eis Workshop, Ges. Mathematik u. Datenverarbeitung MBH*, number 110, March 1986.

[7] T.J. Cockerill, H.Y. Hsieh, J. LeBlanc, D. Ostapko, A.E. Ruehli, J.K. White. Toggle: A circuit analyzer for MOSFET VLSI. *Proc. Int. Conf. VLSI and Computers (COMP-EURO'87) Hamburg, Germany*, May 1987.

[8] C. H. Carlin, A. Vachoux. On partitioning for waveform relaxation time-domain analysis of VLSI circuits. In *IEEE Proc. Int. Symp. on Circuits and Systems (ISCAS)*, pages 701–705, May 1984.

[9] J. White, and A. L. Sangiovanni-Vincentelli. Partitioning algorithms and parallel implementations of waveform relaxation algorithms for circuit simulation. In *IEEE Proc. Int. Symp. on Circuits and Systems (ISCAS)*, pages 1069–1072, June 1985.

[10] A. E. Ruehli,Ed. *Circuit Analysis, Simulation and Design*. Elseviers, North-Holland, New York, Amsterdam, 1987.

[11] K. L. Paap, Y. Han, W.John, B. Klaassen, G.P. Ploger. Concurrent circuit simulation schedules by signal flow graphs. In *International Conference on Computing and Information*, 1989.

[12] M. J. Gander and A.M. Stuart. Space-time continuous analysis of waveform relaxation for the heat equation. *SIAM Journal on Scientific Computing*, 19(6):2014–2031, 1998.

[13] M. J. Gander, L. Halpern, and F. Nataf. Optimal convergence for overlapping and non-overlapping Schwarz waveform relaxation for time dependent problems. In C-H. Lai, P. Bjørstad, M. Cross, and O. Widlund, editors, *Proceedings of the Eleventh International Conference on Domain Decomposition Methods*. ddm.org, 1998. Held in Greenwich, Great Britain, July 20-24, 1998.

[14] A. E. Ruehli and T. A. Johnson. *Circuit Analysis Computing by waveform relaxation*, volume 3. Wiley Encyclopedia of Electrical Electronics Engineering, New York, 1999.

[15] B. Leimkuhler and U. Miekkala and O. Nevanlinna. Waveform relaxation for linear RC circuits. *Impact of Comp. in Science and Engineering*, pages 123–145, 1991.

[16] B. Leimkuhler, A. Ruehli. Rapid convergence of waveform relaxation. *Appl. Numer. Mathematics.*, 11:211–224, July 1993.

[17] Y. L.Jiang, R. M. M. Chen and O. Wing. Convergence analysis of waveform relaxation for nonlinear differential-algebraic equations of index one. *IEEE Transactions on Circuits and Systems*, 47(11):1639–1645, November 2000.

[18] G. D. Gristede, A. E. Ruehli and C. Zukowski. Convergence properties of waveform relaxation circuit simulation methods. *IEEE Transactions on Circuits and Systems*, 45(7):726–738, July 1998.

[19] W. LePage. *Complex variables and the Laplace transform for engineers*. Dover Publications, New York, 1980.

[20] C. Lubich, and A. Osterman. Multi-grid dynamic iteration for parabolic equations. *BIT*, 27:216–234, 1987.

[21] S.Vandevalle. *Parallel Multigrid Waveform relaxation for Parabolic problems*. B. G. Teubner, Stuttgart, Germany, 1993.

[22] F. Nataf and F. Nier. Convergence rate of some domain decomposition methods for overlapping and nonoverlapping subdomains. *Numerische Mathematik*, 75(3):357–77, 1997.

[23] M.J. Gander, L. Halpern, and F. Nataf. Optimal schwarz waveform relaxation for the one dimensional wave equation. *In preparation*, 2002.